The SMEI Real-Time Data Pipeline: From Raw CCD Frames to Photometrically Accurate Full-Sky Maps.

P. Hick[a], A. Buffington[a] and B.V. Jackson[a]

[a]Center for Astrophysics and Space Sciences, University of California San Diego

ABSTRACT

The Solar Mass Ejection Imager (SMEI) records a photometric white-light response of the interplanetary medium from Earth orbit over most of the sky. We present the techniques required to process the SMEI data in near real time from the raw CCD images to their final assembly into photometrically accurate maps of the sky brightness of Thomson scattered sunlight. Steps in the SMEI data processing include: integration of new data into the SMEI data base; conditioning to remove from the raw CCD images an electronic offset (pedestal) and a temperature-dependent dark current pattern; placement ("indexing") of the CCD images onto a high-resolution sidereal grid using known spacecraft pointing information. During the indexing the bulk of high-energy-particle hits (cosmic rays), space debris inside the field of view, and pixels with a sudden state change ("flipper pixels") are identified. Once the high-resolution grid is produced, it is reformatted to a lower-resolution set of sidereal maps of sky brightness. From these we remove bright stars, background stars, and a zodiacal cloud model (their brightnesses are retained as additional data products). The final maps can be represented in any convenient sky coordinate system, *e.g.*, Sun-centered Hammer-Aitoff or "fisheye" projections. Time series at selected sidereal locations are extracted and processed further to remove aurorae, variable stars and other unwanted signals. These time series of the heliospheric Thomson scattering brightness (with a long-term base removed) are used in 3D tomographic reconstructions.

Keywords: Solar Mass Ejection Imager, SMEI, data processing, full-sky observations

1. INTRODUCTION

The Solar Mass Ejection Imager (SMEI) records a photometric white-light response over most of the sky from Earth orbit. The total white-light signal measured by SMEI is the sum of several sources: light from stars and galaxies, scattered sunlight from the zodiacal dust cloud, Thomson-scattered sunlight from free electrons in the solar wind, and auroral light. In addition various kinds of contaminations are present, most notably from cosmic-ray hits, and space debris passing through the field of view. Our primary objective is to isolate the Thomson-scattering signal from electrons in the solar wind across the sky, and use these observations to study the structure and evolution of the solar wind in the inner heliosphere. In the first two years of operation the instrument has recorded the inner heliospheric response to several hundred CMEs, including the May 28, 2003 and the October 28, 2003 halo coronal mass ejections (CMEs). In this preliminary work we present the techniques required to process the SMEI data from the time the raw CCD images become available to their final assembly in photometrically accurate maps of the sky brightness in Thomson brightness relative to a long-term time base.

Processing of the SMEI data includes integration of new data into the SMEI data base as they become available; a conditioning that removes from the raw CCD images an electronic offset (pedestal) and a temperature-dependent dark current pattern; an "indexing" process that places the CCD images onto a high-resolution sidereal grid using known spacecraft pointing information. At this indexing stage further conditioning removes the bulk of the effects of high-energy-particle hits (cosmic rays), space debris inside the field of view, and pixels with a sudden discrete state changes ("flipper pixels").

P.H.: E-mail: pphick@ucsd.edu, Tel. (858) 534-8965;
A.B.: E-mail: abuffington@ucsd.edu, Tel. (858) 534-6630;
B.V.J.: E-mail: bvjackson@ucsd.edu, Tel. (858) 534-3358

Solar Physics and Space Weather Instrumentation, edited by Silvano Fineschi, Rodney A. Viereck,
Proc. of SPIE Vol. 5901, 59011B, (2005) · 0277-786X/05/$15 · doi: 10.1117/12.617996

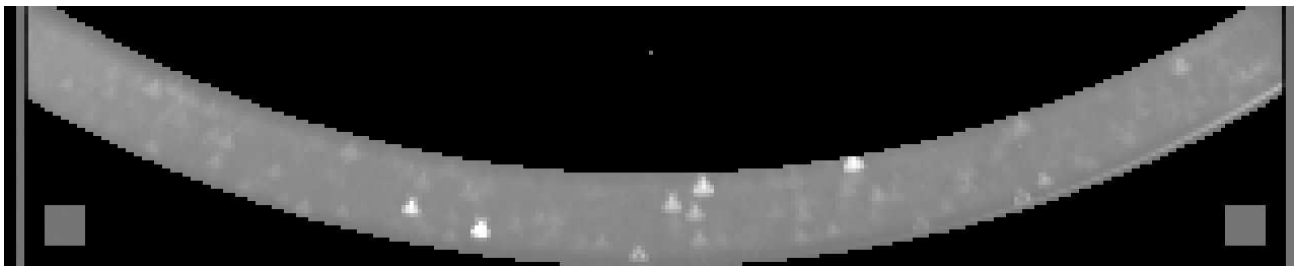

Figure 1. Single 4-second exposure CCD frame from SMEI camera 2 in mode 2 at 2003/02/03 00:43:34 UT. The 60°×3° field of view covers an arc on the CCD. Stars appear as fish-shaped structures, reflecting the PSF of the SMEI optics, on the inner edge, and move radially across the 3° field of view in less than one minute (about a dozen frames). The grey columns on the left and right edge of the frame (each 8 pixels wide and not exposed to outside light) are used in the calculation of pedestal and dark current.

Once the high-resolution grid is produced, it is reformatted to a lower-resolution set of sidereal maps of sky brightness. From these sidereal maps we remove bright stars, background stars, and a zodiacal cloud model (their brightnesses are retained as additional data products). The final maps can be represented in any convenient sky coordinate system. Common formats are Sun-centered Hammer-Aitoff or "fisheye" maps. Time series at selected locations on these maps are extracted and processed further to remove aurorae, variable stars and other unwanted signals. These time series (with a long-term base removed) are used in 3D tomographic reconstructions.

The data processing is distributed over multiple (currently twelve) PCs running Linux, and, runs as much as possible automatically using recurring batch jobs ("cronjobs"). The batch jobs are controlled by Python scripts. The core data processing routines are written in several computer languages: Fortran, C++ and IDL.

2. THE SOLAR MASS EJECTION IMAGER (SMEI)

The Solar Mass Ejection Imager[1,2] is a full-sky, white-light, CCD-based camera system for observing the inner heliosphere from Earth orbit. SMEI was launched into an 840 km Sun-synchronous terminator orbit on January 6, 2003. It shares the Air Force Coriolis Mission spacecraft with the U.S. Navy WindSat instrument. SMEI consists of three cameras, each with a field of view of roughly 60°×3°, aligned in such a way on the spacecraft that combined they image a strip of sky of about 160°×3°. As the spacecraft moves through its polar orbit, the SMEI cameras continuously take 4-second exposures (Figure 1) to sweep out nearly the entire sky over each 102-minute orbit. Images from each orbit are combined to provide a white-light map as visible from Earth orbit (Figure 2). The orbit geometry and the need to keep direct sunlight out of the cameras account for a sunward exclusion zone with a diameter of roughly 20° and a much smaller one in the anti-sunward direction.

SMEI employs never-before attempted baffle and imaging technology that allows photometric observations of the whole sky from Earth orbit[3,4]. Its primary objective is to measure the intensity of Thomson-scattered sunlight from electrons in the solar wind across the sky. This Thomson scattering brightness relates directly to the solar wind density and provides a way to observe and track the interplanetary response of the inner heliosphere to solar disturbances, such as coronal mass ejections. Thus, SMEI provides a means for tracking solar disturbances across the observational gap between near-Sun coronagraphs and near-Earth *in situ* instruments.

The extraction of a photometric measurement of the Thomson scattering intensity by heliospheric electrons from the total observed white light signal requires careful processing to remove contributions from other sources of white light, *e.g.*, from stars and galaxies, the zodiacal dust cloud, and aurorae; contributions from instrumental effects; and contamination of the CCD frames by cosmic rays and space debris. We describe how these factors are being implemented into a data pipeline for processing the SMEI observations, that is capable of producing sky maps of the Thomson scattering brightness to the original photometric specifications of the SMEI design (requiring a differential photometry of 0.1% for each square degree sky bin).

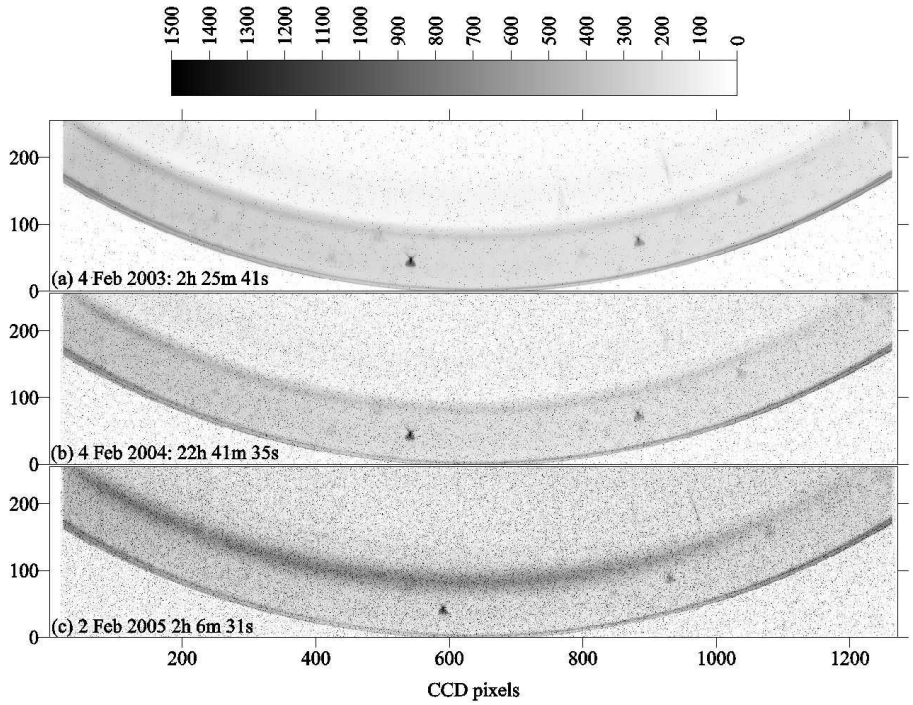

Figure 2. Three raw CCD frames for camera 3 at the indicated times, almost exactly one year apart. The increase over time in the population of "hot" and "flipper" pixels is evident for this camera (in cameras 1 and 2 which run significantly cooler than camera 3 (Section 8) the increase is much less). These same frames, after processing, are shown in Figure 3.

3. INTEGRATION OF NEW DATA

SMEI data are collected from the spacecraft through downlinks to several ground stations (currently Fairbanks, AK, and Svalbaard, Norway). The raw telemetry is initially sent to the National Solar Observatory at Sacramento Peak, NM. Here initial processing takes places in chunks of typically 3-5 hours. The resulting data frames (Figure 1) are then made available to us at UCSD by secure ftp. At UCSD a Python script downloads about 4 GB of raw SMEI frames per day, and automatically integrates the frames into our local SMEI data base. These downloaded data are also stored on DVD for backup purposes. The individual frames are stored on an array of hard drives as compressed FITS files. Presently, 2.5 years into the mission, the data base contains more than 40 million CCD frames stored on six 250 GB hard drives. The data archive is always on line and is accessible through password-protected ftp. On board a single CCD readout has a size of 1272×256 pixels. During normal operations each frame is binned down by the onboard data handling unit to 636×128 (mode 1, mostly used for camera 3) or 318×64 (mode 2, mostly used for cameras 1 and 2) by averaging over 2×2 or 4×4 pixels, respectively. The full size frames (mode 0) are used primarily for calibration purposes, and in particular are taken during weekly calibration runs lasting several orbits.

4. PEDESTAL AND DARK CURRENT

The first step in processing each frame involves the calculation of an electronic offset (pedestal) and dark current. The pedestal is determined from 4-pixel wide columns in the full-size (mode 0) CCD frame (binned to 2 or 1 column in mode 1 or 2, respectively) at the left and right edge of the frame (Figure 1). Similarly, a dark current is determined from 4-pixel wide columns of covered pixels (*i.e.*, shielded from external light sources) neighboring the pedestal columns. Sometimes pixels in these columns contain values far removed from the main distribution of values, *e.g.*, due to cosmic ray hits. These pixels are excluded by using a criterion based on the median: only pixels with values closer to the median than a specific cutoff are used in the pedestal and dark current

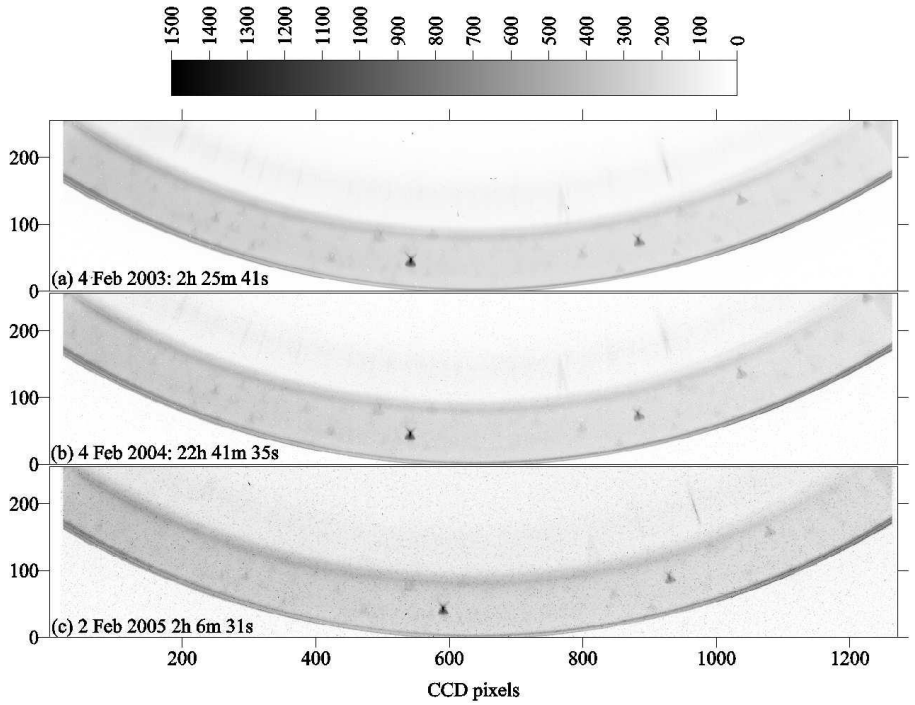

Figure 3. The same three CCD frames as in Figure 2 after processing as explained in Section 4. The use of a "dark current pattern" in particular has proven to be a powerful way to clean up the raw CCD frames, and enables a nearly complete recovery even for the "hot" camera 3. The brightest star in the field of view (near column 600) is HD 218045.

calculation. The cutoff threshold values have been determined empirically; they vary with camera and mode, but are expected to remain the same throughout the mission. For the dark current the median of all pixels meeting the threshold criteria determine the final value for the frame. For the pedestal median and mean are essentially the same, and the mean is used for simplicity.

The electronic offset is removed first by simply subtracting the final mean pedestal for all pixels in the frame. The removal of dark current is more complicated than just subtracting a single value from the entire CCD frame. Instead, weekly calibrations in mode 0 of one orbit duration obtained with shutter[1] closed, are used to determine a dark current "pattern": a group of clean CCD frames (*i.e.*, free of contamination by cosmic ray hits) are selected from the calibration data and, after subtraction of their pedestals, are averaged together to create the pattern, and an associated single "pattern dark current". A data base of these calibration patterns is maintained as closed shutter calibration data become available. Subtraction of the dark current for open shutter frames involves subtraction of the pattern scaled by the ratio of its dark current and the pattern dark current.

The pattern accounts for two effects: the build-up of dark current over the read-out time of the CCD frame (the 1st pixel in the read-out has a smaller dark current than the last), and systematic differences between pixels ("hot" pixels, and "flipper" pixels). Figures 2 and 3 show three mode 0 frames from camera 3 taken almost exactly one year apart before and after processing.

The mean pedestal and dark current for each frame, together with the appropriate pattern to be used, is determined separately for each frame in the SMEI data base, and is added to the FITS header for each CCD frame. At this stage also other useful information is added to the frame. In particular this includes two angles defining the position of the Sun relative to the camera optical axis, the equatorial coordinates of the three brightest objects in the sky (Sun, Moon and Venus), and one or more quality indicators to indicate whether or not to exclude frames for further processing.

5. MAPPING TO A SIDEREAL GRID

All frames collected over a single orbit (about 1500 for each camera) combine to form one full-sky map. The composition is achieved using an hierarchical triangular mesh (HTM[5]) grid with an angular resolution of about 0.1°. The HTM grid covers the celestial sphere in triangular bins that, within acceptable limits (about a factor of two), have the same area, and hence does not suffer from the strong edge deformations inherent in common planar map projections of the celestial sphere.

All pixels of all frames are "indexed" by placing them in the appropriate triangles in the HTM grid. Each CCD pixel of about 0.05° on the sky in mode 0 (0.1° in mode 1, and 0.2° in mode 2) contributes to several HTM triangles. Each sidereal location in the sky (*i.e.*, each HTM triangle) receives contributions from a sequence of subsequent frames taken as the camera field of view sweeps across the sidereal location. This combination of contributions from the time domain provides a fortuitous but elegant means of detecting temporally isolated spikes in the CCD frames, such as cosmic ray hits (isolated high values in one or more pixels in a single frame) and space debris (traveling across the field of view in times short compared to the exposure time). Thus, in addition to preparing the full-sky sidereal maps, the indexing phase also is our main defense against these short-lived contaminations in the data.

Once the indexing is completed and a full-sky HTM grid is assembled, a planar representation of the sky map is made using a conventional equatorial grid (right ascension and declination) with a resolution of 0.2°. This representation consists of three maps: a rectangular map for the equatorial region between -60° and +60° declination, and two polar projections for the north polar region above +50° declination and the south polar region below -50° declination.

These orbital maps are constructed separately for each of the three SMEI cameras. A data base of orbital maps consists of FITS files containing the three above-mentioned maps. For each orbit separate FITS files are maintained for each camera, with one additional FITS file for the three cameras combined.

Further processing of these orbital maps primarily involves the removal of remaining "unwanted" (from the perspective of heliospheric solar wind studies) white light signals. Once the contribution is determined, results are saved to support other scientific studies, prior to removing them as the next step to isolating the heliospheric signal. First we deal with contributions from stars, galaxies, *etc.*, consisting of point-like bright stars and planets, and a diffuse background from faint stars (primarily the Milky Way, Figure 4).

6. REMOVAL OF STARS

To maintain the required photometric precision point-like objects brighter than 6^{th} magnitude (stars and the brightest planets) need to be removed individually[6]. A spin-off product of the star removal will be photometric stellar time series with time resolution of 102 minutes (the orbital period)[7]. Fainter background stars (including the diffuse Milky Way) are removed by subtracting a background sky map built from SMEI observations of the anti-solar hemisphere. After removal of the star signal the resulting skymaps are saved in the same format (FITS files with a rectangular equatorial and two polar maps) as the original orbital maps.

7. REMOVAL OF ZODIACAL LIGHT

One of the brightest diffuse signals observed by SMEI is zodiacal light brightness (sunlight reflected from the zodiacal dust cloud). This must be modeled accurately and removed from the SMEI sky maps to provide the heliospheric contributions free from otherwise large changes in the background. We currently have a provisional technique to determine the zodiacal light brightness from the SMEI maps, which assumes that, except for a tilt relative to the ecliptic plane, the brightness distribution has both north-south and east-west symmetry. As a byproduct this provides a measure of the orientation of the plane of the dust cloud relative to the ecliptic plane, as well as the Gegenschein brightness throughout the year[8]. Zodiacal brightness calculations are best performed in sun-centered ecliptic coordinates (as opposed to the star subtraction which is done in a sidereal equatorial reference frame).

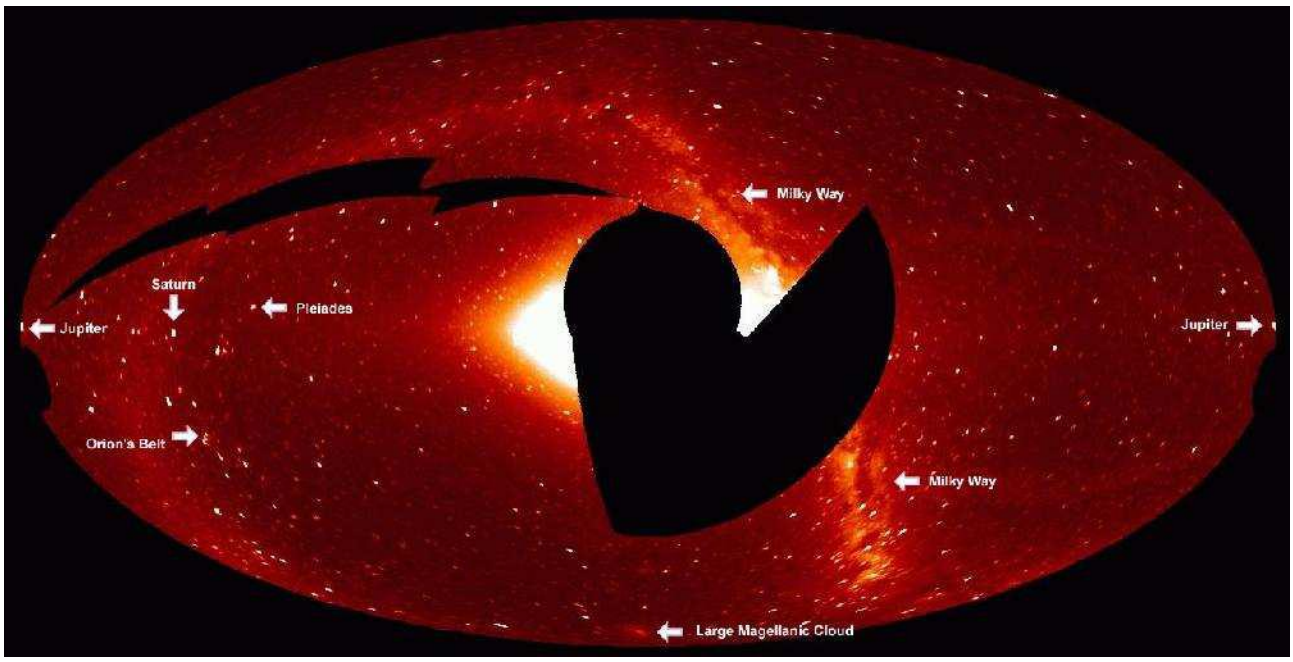

Figure 4. Sky map in Hammer-Aitoff projection constructed from individual SMEI CCD frames. A typical composite map consists of ~4500 individual frames (1500 from each camera). The Sun is at the center; the ecliptic plane is along the horizontal axis. Various objects are labeled. Blank areas include the exclusion zones in the solar and anti-solar directions; areas not observed because the Sun was too close to camera 3 (pointing closest to the Sun) and its shutter was closed; and areas too contaminated by radiation belt particle hits (the slash along the upper left).

8. SOME OTHER PROBLEMS

Several additional data analysis complications exist which have been partly addressed.

A serendipitous discovery of SMEI was the presence of aurorae at altitudes higher then 840 km[9,10]. These aurorae are observed fairly often when SMEI crosses the auroral ovals, and are particularly strong when a geo-effective CME hits Earth. A procedure exists to remove these aurorae from the data[11].

Camera 3 (pointing closest to the Sun) runs at a significantly higher temperature than the other two cameras, causing such fast changes in the population of "flipper pixels" that updates to the calibration patterns are needed every orbit to supplement the weekly closed shutter patterns.

For cameras 2 and 3 a "glare" is seen near the outer edges of the field of view whenever the Sun is close[4]. Reference maps of this glare are now available. The glare is removed by subtracting this reference map scaled by a single value determined by the position of the Sun relative to the optical axis of the camera.

9. TOMOGRAPHIC STUDY OF CMES

One of the most important studies for the final clean heliospheric Thomson-scattering signal is the study of the characteristics and evolution of solar disturbances, such as CMEs. We have a tomographic technique capable of reconstructing CME densities in 3D. So far this technique has been applied to two major CMEs observed with SMEI using primarily time series extracted from sidereal locations in the orbital skymap away from bright stars[11].

ACKNOWLEDGMENTS

This work was supported by NASA Grants NAG5-11906 and NAG5-134543; and USAF grant AF49620-01-1-0054. SMEI was designed and constructed by a team of scientists and engineers from the U.S. Air Force Research

Laboratory, the University of California at San Diego, Boston College, Boston University, and the University of Birmingham in the U.K. Financial support was provided by the Air Force, the University of Birmingham, and NASA.

REFERENCES

1. Eyles, C.J., G.M. Simnett, M.P. Cooke, B.V. Jackson, A. Buffington, P.P. Hick, N.R. Waltham, J.M. King, P.A. Anderson, and P.E. Holladay, "The Solar Mass Ejection Imager (SMEI)", Solar Phys. **217**, 319-347, 2003.
2. Jackson, B.V., A. Buffington, P.P. Hick, R.C. Altrock, S. Figueroa, P.E. Holladay, J.C. Johnston, S.W. Kahler, J. Mozer, S. Price, R.R. Radick, R. Sagalyn, D. Sinclair, G.M. Simnett, C.J. Eyles, M.P. Cooke, S. J. Tappin, T. Kuchar, D. Mizumo, D.F. Webb, P. Anderson, S.L. Keil, R.E. Gold, and N.R. Waltham, "The Solar Mass Ejection Imager (SMEI) mission", Solar Phys. **225**, 177-207, 2004.
3. Buffington, A., Jackson, B.V. and Hick, P.P., "Calculations for and laboratory measurements of a multistage labyrinthine baffle for SMEI", Proc. SPIE **4853**, 490-503, 2003.
4. Buffington, A., Jackson, B.V. and Hick, P., "Space performance of the multistage labyrinthine SMEI baffle", these proceedings, 2005.
5. Kunszt, P.Z., Szalay, A.S., Csabai, I. and Thakar, A.R., "The Indexing of the SDSS Science Archive", Proc. ADASS IX, eds. N. Manset, C. Veillet, D. Crabtree, ASP Conf. Series **216**, 141, 2000 (http://www/sdss.jhu.edu/htm).
6. Buffington, A., Smith, A.C., Jackson, B.V., and Hick, P., "Photometric Calibration for the Solar Mass Ejection Imager (SMEI)", BAAS Vol. 36, Abstract 10.07, p. 1350, 2005.
7. Buffington, A., Jackson, B.V., Hick, P.P., Penny, A., and Simnett, G.M., "The Solar Mass Ejection Imager (SMEI) and its potential as a precision time-series photometer", BAAS Vol. 36 (2), Abstract 69.10, p. 795, 2004.
8. Simon, S., Jackson, B.V., Buffington, A., Hick, P.P. and Smith, A.C., "Zodiacal Light Analysis and Removal From the Solar Mass Ejection Imager (SMEI) Data", EOS Trans. AGU **85 (47)**, Fall Meet. Suppl., Abstract SH21A-0398, 2004.
9. Mizuno, D.R., "Observations of High Altitude Aurorae With the Solar Mass Ejection Imager", EOS Trans. AGU **85 (47)**, Fall Meet. Suppl., Abstract SH11A-06, 2004.
10. Mizonu, D.R., A. Buffington, M.P. Cooke, C.J. Eyles, P.P. Hick, P.E. Holladay, B.V. Jackson, J.C. Johnston, T.A. Kuchar, J.M. Mozer, S.D. Price, R.R. Radick, G.M. Simnett, D. Sinclair and D.F. Webb, "Very High Altitude Aurorae Observations with the Solar Mass Ejection Imager", J. Geophys. Res, *in press*, 2005.
11. Jackson, B.V., Buffington, A., Hick, P.P., Yu, Y. , Webb, D., Mizuno, D., and Kuchar, T.,, "Preliminary Three Dimensional CME Mass and Energy Using Solar Mass Ejection Imager (SMEI) Data", Eos Trans. AGU, **86 (18)**, Jt. Assem. Suppl., Abstract SP44A-05, 2005.